Vibrational Spectroscopy 70 (2014) 28–35

Contents lists available at ScienceDirect

Vibrational Spectroscopy

journal homepage: www.elsevier.com/locate/vibspec

Matrix isolation studies of carbonyl selenide, OCSe: Evidence of the formation of dimeric species, $(OCSe)_2$

Jovanny A. Gómez Castaño [1], Rosana M. Romano *

CEQUINOR (UNLP-CONICET), Departamento de Química, Facultad de Ciencias Exactas, Universidad Nacional de La Plata, 47 esq. 115, 1900 La Plata, Argentina

ARTICLE INFO

Article history:
Received 29 July 2013
Received in revised form 25 October 2013
Accepted 25 October 2013
Available online 1 November 2013

Keywords:
Matrix isolation
IR spectroscopy
Dimers
Carbonyl selenide
Photochemistry

ABSTRACT

OCSe isolated in solid Ar or N_2 at 10 K was investigated by FTIR spectroscopy. The IR spectra of OCSe diluted in a 1:1000 proportion with the matrix gases were interpreted in terms of monomeric carbonyl selenide in a single matrix site. The IR spectra of more concentrated matrices revealed several new IR absorptions, which were tentatively assigned to different dimeric structures, aided by the prediction of quantum chemical calculations. The different matrices were exposed to UV–visible broad-band radiation, finding that monomeric OCSe decomposes into CO and Se, as evidenced by the IR absorption of CO perturbed by the presence of a selenium atom in the same matrix cage, while dimeric forms of OCSe decompose giving mainly $(CO)_2$.

1. Introduction

Carbonyl selenide, a relatively unstable linear triatomic molecule, has been the subject of several investigations using different experimental and theoretical techniques. Its structural and spectroscopic properties were determined using vibrational [1–5], microwave [6,7], UV–visible [8,9] and photoelectron [10,11] spectroscopies. Reports on the induced fluorescence photodissociation of OCSe [12–15] were motivated in the evaluation of selenium systems as precursors for energy-storage lasers. The photolysis, either in gas phase using laser radiation [16,17] or in solid phase isolated in Xe or trans-2-butene at 77 K using a medium pressure mercury lamp [18], has also been investigated.

More recently, novel compounds with general formula XC(O)SeY, with X, Y = halogen, have been isolated through matrix photochemical reactions between OCSe and F_2 [19], Cl_2 [20], Br_2 [20] and ClF [21]. In these matrix reactions, the formation of pre-reactive molecular complexes between carbonyl selenide and dihalogen molecules has been proposed to play an important role as the initiators of photochemical reactions. Due to the high dilution of the reactants in the inert matrix gases – usually below 1:200 – the probability of the reactions increases if it is possible to trap the two reactants together in the form of molecular complexes. The geometry of these molecular complexes can determine the direction of the photochemical reaction. For example, the intermediacy of the van der Waals complex O=C=Se···F–F favoured the formation of *anti*-FC(O)SeF in the first place, which was then transformed, through a randomization process, into *syn*-FC(O)SeF [19]. The formation of 1:1 molecular complexes between two molecules competes with the formation of the corresponding dimeric species. Therefore, a detailed study of the photochemical reaction mechanism between OCSe and XY requires understanding of the energetics and geometries of the dimers of the reactants, but also their spectroscopic properties, allowing their identification during the reactions.

Although the dimers of the congeners CO_2 and OCS have stimulated several investigations during the last decades [22–34], there are no reports in the literature – as far as we know – as to the dimeric structures of carbonyl selenide, $(OCSe)_2$. The structure of $(OCO)_2$ was the subject of controversy between two possible forms: a T-shaped structure possessing C_{2v} symmetry, and a parallel structure slightly slipped with C_{2h} symmetry. IR gas-phase [22] and matrix-isolation studies [23] have proposed the T-shaped form. However, later investigations have been interpreted in terms of a slightly slipped parallel structure [24,25]. In a more recent study of carbon dioxide dimer isolated in argon and nitrogen matrices through FTIR spectroscopy, a complete assignment of the fundamental and non-fundamental IR absorptions of the slightly slipped parallel structure was presented. In addition, the bonding properties of the $(CO_2)_2$ complex have been interpreted by a natural bond orbital (NBO) analysis in terms of 'donor–acceptor' interactions [26].

* Corresponding author. Tel.: +54 2214259485; fax: +54 2214259485.
E-mail address: romano@quimica.unlp.edu.ar (R.M. Romano).
[1] Present address: Escuela de Ciencias Químicas, Facultad de Ciencias, Universidad Pedagógica y Tecnológica de Colombia (UPTC), Avenida Central del Norte, 150003 Tunja, Boyacá, Colombia.

0924-2031/$ – see front matter © 2013 Elsevier B.V. All rights reserved.
http://dx.doi.org/10.1016/j.vibspec.2013.10.005

Similarly, several studies of the dimeric forms of OCS were reported. An early investigation of the structure of $(OCS)_2$ has postulated a form with both OCS sub-units side-by-side, although it was ambivalent as to the non-polar antiparallel structure with C_{2h} symmetry or the C_s polar parallel form [27]. The most stable structure of $(OCS)_2$, definitively determined by the analysis of its infrared spectrum, was shown to have a planar centrosymmetric structure with slipped antiparallel OCS monomers with C_{2h} symmetry [29]. *Ab initio* calculations of the structure of (OCS)2 at MP2 level concluded that the experimentally observed geometry is indeed the lowest energy form, and also found three other stationary points located 74, 107 and 152 cm^{-1} higher in energy than the most stable structure[30]. In order of binding energy, these correspond to a slipped parallel structure (C_s), an antiparallel form (C_{2h}) and a structure with the two monomers collinear ($C_{\infty v}$), respectively. The polar isomer of OCS dimer with a slipped and approximately parallel structure was detected by infrared spectroscopy [31], and afterwards confirmed by microwave spectroscopy [32]. Recently, a new intermolecular potential energy surface was reported for the OCS dimer [33]. In addition to the structures mentioned above, a cross-shaped isomer was found only 100 cm^{-1} above the global minimum. A complete review of the theoretical structures, potentials and spectroscopic properties of dimers, trimers and large clusters of linear molecules (CO_2, OCS, CS_2, N_2O, and C_2H_2) has recently been reviewed [33].

In this paper we present experimental evidence of dimeric forms of carbonyl selenide, revealed by the FTIR spectra of matrix isolated samples in different proportions. The comparison between the experimental and theoretical IR shifts of the dimeric forms with respect to the monomer has been used to assist assignment of the bands to the different dimers. If only for the purpose of clarity, the theoretical results describing the optimized geometries of different $(OCSe)_2$ forms, their energy differences and vibrational and bonding properties, are presented in the first part of Section 3. These results are then used as a starting point for the interpretation of the experimental FTIR spectra of OCSe isolated in solid matrices in terms of the different dimeric forms. The matrices were exposed to UV–visible broad-band photolyzing radiation, and the decomposition mechanisms for the monomer and dimeric species were proposed.

2. Experimental and theoretical methods

The OCSe was prepared according to the two stages reaction reported by Kondo et al. [35] by passing a low flow of pure CO (approx. 30 mL/min) through a solution of metallic grey selenium (Aldrich) and *n*-butylamine in dry THF for 2 h at ambient temperature. The formed colourless adduct solution was then carefully added to a 1:8 mixture of sulphuric acid and THF at −78 °C in vacuum conditions. Subsequent repeated trap-to-trap distillations in a vacuum line from the reaction vessel at −50 °C resulted in pure OCSe. The purity of the OCSe was checked by its gas phase IR spectrum [1] using a gas cell with an optical path of 10 cm in a Bruker-Equinox 55 FTIR-spectrometer (the FTIR spectrum of the distilled OCSe with its prominent sharp intense C=O vibration at 2010 cm^{-1} can be observed in Fig. S1 of the Supplementary Material). The Ar and N_2 matrix gases (both AGA) were passed through a trap cooled to −80 °C to retain possible traces of impurities.

Gas mixtures of OCSe with Ar at the proportions 1:1000, 1:500, 1:200 and 1:100 and with N_2 in the proportions 1:1000 and 1:200 were prepared by standard manometric methods. Such mixtures were then deposited on a CsI window cooled at 10 K by means of a displex closed cycle refrigerator (SHI-APD Cryogenics, model DE-202) using the pulsed deposition technique [36,37]. The IR spectra of each matrix sample were recorded at resolutions of 0.5 cm^{-1} and 0.125 cm^{-1}, with 256 scans, using a Nexus Nicolet instrument equipped with either an MCTB or a DTGS detector (for the ranges 4000–400 cm^{-1} or 600–180 cm^{-1}, respectively). Following deposition and the IR analysis of the resulting matrix, the sample was exposed to broad-band UV–visible radiation ($200 \leq \lambda \leq 800$ nm) from a Spectra-Physics Hg–Xe arc lamp operating at 1000 W. The output from this lamp was limited by a water filter to absorb IR radiation and so minimize any heating effects.

The quantum computational calculations were performed using the Gaussian program package G03 [38]. With the aim of predicting the possible OCSe dimer structures, several potential energy surface scans were performed, varying both distances and angles simultaneously. Using the energy minima found during the scans as starting values, full geometry optimizations with the simultaneous relaxation of all the geometric parameters were performed, and followed by vibrational frequency calculations to ascertain that the optimized structures corresponded to genuine minima. The interaction energies were computed and corrected for a basis set superposition error (BSSE) [39] using the counterpoise correction procedure proposed by Boys and Bernardi [40], and for zero-point energy differences.

3. Results and discussion

3.1. Theoretical calculations of the dimeric structures of OCSe

3.1.1. Equilibrium geometries

Different bi-dimensional potential energy scans were performed in order to find the energy minima for the $(OCSe)_2$ system using the B3LYP/6-31+G* approximation. In the first place, the search was restricted to planar structures assuming that, in a planar arrangement, the possibility of interaction between the two units would be enhanced, and also taking into consideration the known structures of the related $(OCO)_2$ and $(OCS)_2$ species. The intermolecular distance R and the angle α formed between the two subunits, defined in Fig. 1, were varied simultaneously. As a result, several structures were found to correspond to minima over the energy surfaces. Each of these structures was later optimized with the MP2/aug-cc-pVDZ method and the frequencies calculated with the same level of approximation. Only five structures, depicted in Fig. 1, have remained as stable forms, as some of the others converged on one of these five structures or else corresponded with transition states, for which the vibrational spectra present one imaginary frequency. Taking into consideration the recently reported cross-shaped isomer of $(OCS)_2$ [33], this form was investigated for $(OCSe)_2$. Any attempt to optimize the cross-shaped structure of the OCSe dimer has failed, since the geometry converged on the corresponding of dimer I of Fig. 1.

A complete list of the calculated parameters of the five planar structures (dimers I–V) is located in the Supplementary Material (Table S1), while the intermolecular distances R, the intermolecular angles and the penetration distances d_p, defined as the difference between the sum of the van der Waals radii of the interacting atoms and the equilibrium interatomic distance in the complex [41], are presented in Table 1. The forms I and III present a slipped antiparallel structure with C_{2h} symmetry, in coincidence with the reported structure for $(CO_2)_2$ [26]. The difference between dimer I and III is that in the first case the selenium atom of each unit interacts with the C=O group of the other unit, while in the second case it is the oxygen atom of one unit that interacts with the C=O group of the other. Dimer II presents a slipped quasi-parallel structure and dimer IV an angular arrangement between the two subunits, both with C_s symmetry. The last structure, called 'dimer V', is linear with the oxygen atom of one of the subunits interacting with the selenium atom of the other subunit, and presents $C_{\infty v}$ symmetry. Four

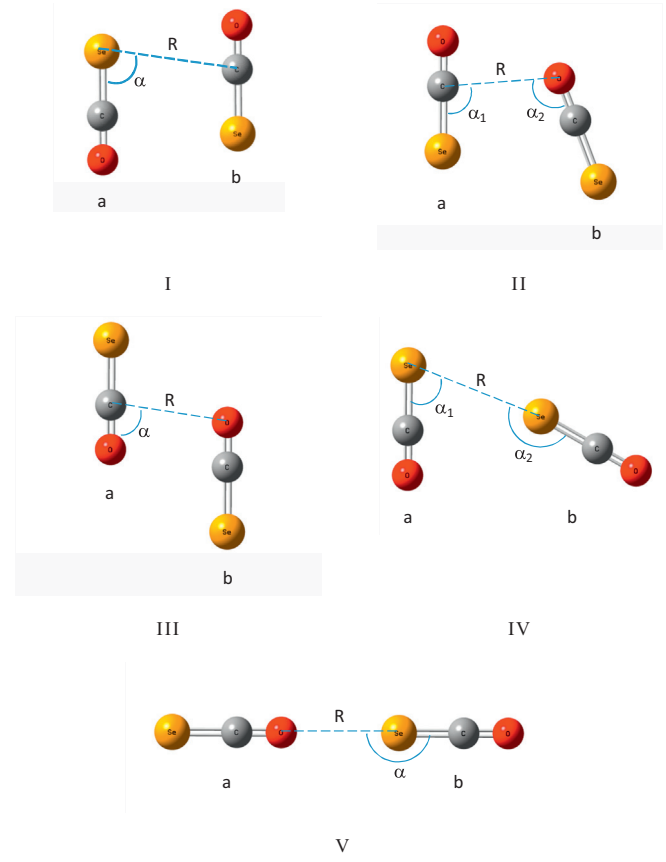

Fig. 1. Optimized structures for the dimers of OCSe calculated with the MP2/aug-cc.pVDZ approximation: (I) slipped antiparallel structure with C_{2h} symmetry, (II) slipped quasiparallel structure with C_s symmetry, (III) slipped antiparallel structure with C_{2h} symmetry, (IV) angular structure with C_s symmetry, and (V) linear structure with $C_{\infty v}$ symmetry.

of these five structures, I, II, III and V, are in agreement with the theoretical structures reported for the dimeric species of carbonyl sulphide, $(OCS)_2$ [30–32].

3.1.2. Vibrational spectra

The vibrational frequencies of the dimeric species depicted in Fig. 1 were calculated with the MP2/aug-cc-pVDZ approximation to characterize each of them as a true energy minima, and also to predict the frequency shifts of the vibrational modes of the dimers with respect to the monomer, which provides a basis for comparison with the results obtained from the matrix-isolation experiments.

The vibrational spectrum of monomeric OCSe is characterized by 3N – 5 = 4 normal modes, that can be described as the C=O stretching mode ($\nu_{C=O}$), the C=Se stretching mode ($\nu_{C=Se}$), and the doubly degenerated bending mode, δ_{OCSe}. On the other hand, the vibrational spectra of the dimeric forms of OCSe are composed of 3N – 6 = 12 (for structures I–IV) or 3N – 5 = 13 (for structure V) normal modes. Eight of these modes correspond to intra-molecular modes, while the remaining ones are related to inter-molecular vibrations. These latter modes are below the experimental spectral range, and for this reason will not be discussed here. As shown in Table 2, in which the calculated wavenumbers and relative intensities of the intra-molecular modes of each of the dimeric structures of OCSe are listed, the theoretical spectrum strongly depends on the symmetry of the dimer. In structures I and III – which possess C_{2h} symmetry – only one vibrational mode is expected in the carbonyl region of the IR spectra, corresponding to the in-phase stretching vibration of both C=O groups. In the C=Se stretching region, only one mode is also predicted, but with much less intensity than the former (the theoretical intensity ratio between $\nu_{C=O}$ and is $\nu_{C=Se}$ is 100:1). On the other hand, in the simulated IR spectra of structures II and IV, belonging to the C_s group, and structure V, with $C_{\infty v}$ symmetry, all the absorptions are IR-active, giving more complex IR spectra.

Table 1
Intermolecular distances (in Å), intermolecular angles (in degrees), sum of the van der Waals radii and penetration distances of the equilibrium dimer structures calculated with the MP2/aug-cc-pVDZ approximation.

Dimer	R^a	α^a	$d_p{}^b$
I	3.643	82.0	−0.04
II	3.112	94.7 (α_1) 106.5 (α_2)	0.11
III	3.139	81.7	0.08
IV	3.764	69.5 (α_1) 171.4 (α_2)	0.04
V	3.123	180.0	0.48

[a] Defined in Fig. 1.
[b] $d_p = \sum r_{vdW} - R$, where $\sum r_{vdW}$ is the sum of van der Waals radii from Ref. [39].

3.1.3. Interaction energies

The binding energies, ΔE, for each of the dimeric structures depicted in Fig. 1 were calculated using the correction proposed by Nagy et al. [39], which takes into account the counterpoise-corrected binding energies due to the error of the basis set superposition [40], ΔE^{CP}, and the term GEOM that accounts for the changes of geometry experienced by the free OCSe monomers on dimerization. The values ΔE^{CP} calculated with the MP2/aug-cc-pVDZ theoretical approximation are presented in Table 3, while the uncorrected binding energies and the BSSE and GEOM terms are presented as the Supplementary Material in Table S2. The five structures are predicted to be energetically more stable than the monomers, being of the theoretical stability order II > I > V ≈ IV ≈ III (see Table 3).

3.1.4. NBO analysis

The bonding properties of the complexes have been interpreted by a Natural Bond Orbital (NBO) analysis in terms of 'donor–acceptor' interactions [42]. In all the $(OCSe)_2$ systems studied, the most important orbital stabilization interaction occurs in the molecular plane between one of the non-bonding orbitals of the Se or O atoms of one of the sub-units and the unoccupied σ^* or π^* orbitals of the other subunit. The net charge transferred, q, and the energy reduction, $\Delta E^{(2)}{}_{n\rightarrow\sigma^*/\pi^*}$, are included in Table 3. Fig. 2 shows a schematic representation of the orbital interaction for dimers I–V of OCSe. For the symmetric structures I and III, the most important contribution to the stabilization of the dimer arises from an interaction of a non-bonding orbital of the Se atom (dimer I) or the O atom (dimer III) of one of the OCSe unit with a π^*(C=O) orbital of the other OCSe unit. In these highly symmetric structures, each of the OCSe molecules can act simultaneously as donor and acceptor, giving a double interaction and a null total charge transferred.

In the slipped quasi-parallel structure (dimer II), the strongest orbital interaction occurs from a non-bonding orbital of the Se atom of the OCSe molecule labelled as "a" in Figs. 1 and 2 to a π^*(C=O) orbital of the "b" unit (see Fig. 2II-A). Another contribution arises from a charge transfer of the π(C=O) bonding orbital of the OCSe "b" to the π^*(C=O) of the "a" unit. This interaction is reflected in a slight increase in the C=O distance of the "b" OCSe molecule of dimer II with respect to the same parameter in the monomer (see Table S1).

The stabilization of the angular structure IV can also be explained through two different interactions, one from the non-bonding orbital of a Se atom of the "a" moiety to the σ^*(C=O) orbital of the "b" OCSe unit, and the other from the non-bonding orbital of

Table 2
Calculated wavenumbers (in cm^{-1}) and IR relative intensities (between parenthesis) of different dimers of OCSe using the MP2/aug-cc-pVDZ approximation.

Dimer I		Dimer II		Dimer III		Dimer IV		Dimer V		Vibrational mode
ν	$\Delta\nu$[a]	ν	$\Delta\nu$[a]	ν	$\Delta\nu$[a]	ν	$\Delta\nu$[a]	ν	$\Delta\nu$[a]	
2004.9[b] (100)	10.6	2001.4[c] (100)	7.1	1992.3[b] (100)	−2.0	1995.8[b] (45)	1.5	1994.3[b] (4)	0.0	ν(C=O)
1978.8[c] (0)	−15.5	1985.5[b] (6)	−8.8	1991.5[c] (0)	−2.8	1989.4[c] (100)	−4.9	1985.8[c] (100)	−8.5	ν(C=O)
683.5[c] (0)	0.1	685.1[c] (<1)	1.7	685.9[b] (1)	2.5	680.7[b] (<1)	−2.7	690.4[d] (<1)	7.0	ν(C=Se)
683.0[b] (1)	−0.4	681.5[b] (<1)	−1.9	685.6[c] (0)	2.3	676.8[c] (<1)	−6.6	679.6[e] (<1)	−3.8	ν(C=Se)
469.9[b] (0)	1.4	468.6[c] (<1)	0.1	469.6[c] (<1)	1.1	472.9[c] (<1)	4.4	476.1[b] (<1)	7.6	δ(OCSe)
468.0[c] (<1)	−0.5	468.1[b] (<1)	−0.4	469.1[b] (0)	0.6	472.9[c] (<1)	4.4	476.1[b] (<1)	7.6	δ(OCSe)
462.9[c] (<1)	−5.6	464.8[b] (<1)	−3.7	467.6[b] (0)	−0.9	466.7[b] (<1)	−1.8	469.8[c] (<1)	1.3	δ(OCSe)
462.1[b] (0)	−6.4	460.6[c] (<1)	−7.9	464.4[c] (<1)	−4.1	465.4[b] (<1)	−3.1	469.8[c] (<1)	1.3	δ(OCSe)

[a] $\Delta\nu = \nu$ (dimer) − ν (free OCSe).
[b] Out-of-phase.
[c] In-phase.
[d] OCSe-a.
[e] OCSe-b.

a Se atom of the "b" OCSe to the π*(C=O) orbital of the "a" OCSe unit (see Fig. 2IV-A and IV-B, respectively). The most important contribution to the stabilization energy in the dimeric structure V can be assigned to a charge transfer from a non-bonding orbital of a Se atom of the "a" unit to the σ*(C=Se) orbital of the other OCSe molecule.

3.2. Matrix-isolation experiments

3.2.1. Monomer of OCSe

Mixtures of OCSe and Ar or N_2 in different proportions were studied by FTIR matrix-isolation spectroscopy. The FTIR spectrum of OCSe diluted in solid argon in a proportion of 1:1000 was interpreted in terms of monomeric carbonyl selenide, isolated in an asymmetrical matrix site. Table 4 lists all the IR absorptions observed in the spectra of OCSe isolated in solid Ar or N_2 in the proportion 1:1000, together with the proposed assignment. Since, as far as we know, there were no previous reports in the literature of OCSe isolated in solid matrices, we have included in the table the IR wavenumbers of a gaseous sample of carbonyl selenide for the purpose of comparison.

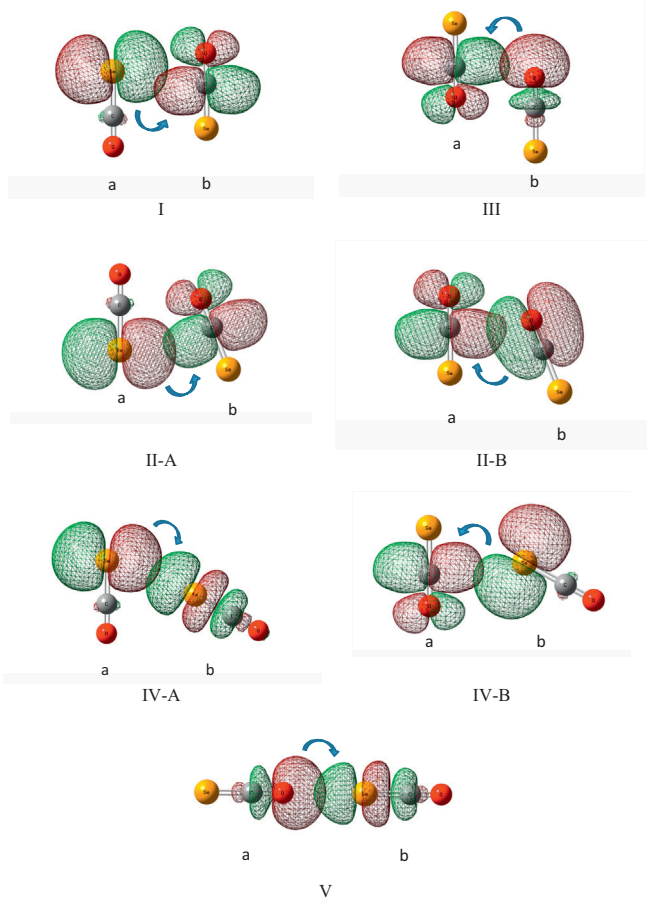

Fig. 2. Schematic representation of the orbital interactions for dimers I–V of $(OCSe)_2$.

Table 3
Calculated counterpoise-corrected binding energies, ΔE^{CP}, net charge transferred, q, and orbital stabilization of the dimers of OCSe using the MP2/aug-cc-pVDZ theoretical approximation.

Dimer	ΔE^{CP} (kcal/mol)	q (e)	$\Delta E_{n\rightarrow\sigma^*/\pi^*}$ (kcal/mol)
I	−1.71	0	−0.62
II	−2.21	0.001	−1.58
III	−1.21	0	−0.29
IV	−1.26	0.006	−1.57
V	−1.29	0.002	−1.48

Table 4
Wavenumbers (in cm^{-1}) and assignment of the IR absorptions of OCSe isolated in solid Ar or N_2.

Ar matrix	N_2 matrix	Vapour IR[a]	Assignment[b]
3994.8		4023	$2\nu_1$ OCSe
3288.5		3303	$\nu_1 + 2\nu_3$ $OC^{80}Se$
2656.0			$\nu_1 + \nu_3$ $OC^{76}Se$
2654.8			$\nu_1 + \nu_3$ $OC^{77}Se$
2653.7			$\nu_1 + \nu_3$ $OC^{78}Se$
2651.6	2653.7	2666	$\nu_1 + \nu_3$ $OC^{80}Se$
2649.5			$\nu_1 + \nu_3$ $OC^{82}Se$
2009.0	2015.5	2023	ν_1 OCSe
1969.6	1975.4		ν_1 ^{18}OCSe
1959.8	1966.1		ν_1 $O^{13}CSe$
1286.7			$2\nu_3$ $OC^{78}Se$
1282.4		1283	$2\nu_3$ $OC^{80}Se$
933.4	937.4	928	$2\nu_{2\,(I)}$ OCSe[c]
929.8			$2\nu_{2\,(II)}$ OCSe[c]
648.1			ν_3 $OC^{76}Se$
647.0			ν_3 $OC^{77}Se$
646.0			ν_3 $OC^{78}Se$
643.9	640.4	644	ν_3 $OC^{80}Se$
641.8			ν_3 $OC^{82}Se$
466.0	461.2	463	$\nu_{2\,(I)}$ OCSe[c]
464.3			$\nu_{2\,(II)}$ OCSe[c]

[a] From Ref. [1].
[b] ν_1, ν_2 and ν_3 are assigned to $\nu_{C=O}$, δ_{OCSe} and $\nu_{C=Se}$, respectively.
[c] I and II refers to the different absorptions assigned to the deformation OCSe vibrational mode as a consequence of the loss of degeneracy due to the matrix site effect.

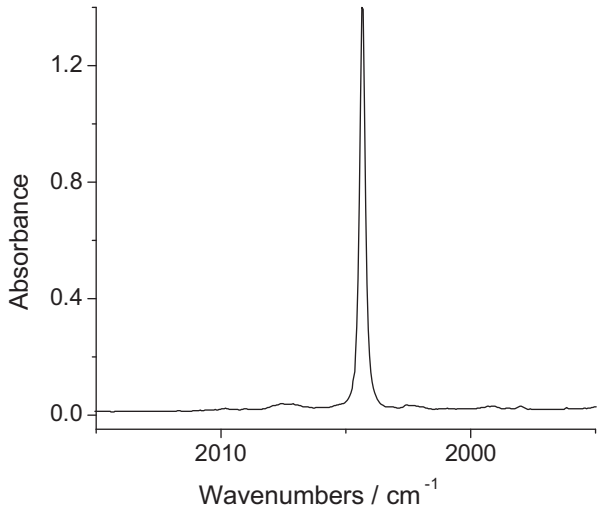

Fig. 3. FTIR spectra in the νC=O spectral region of OCSe isolated in Ar matrix in 1:1000 proportion.

3.2.1.1. The $\nu_{C=O}$ region. The IR spectrum of a mixture of OCSe:Ar 1:1000 at 10 K is dominated by a unique narrow absorption at 2009.0 cm^{-1}, as presented in Fig. 3, indicating the presence of only one matrix site. Satellites at 1969.6 and 1959.8 cm^{-1}, with relative intensities with respect to the 2009.0 cm^{-1} absorption of approximately 0.2% and 1%, have been assigned to the $\nu(C=^{18}O)$ and $\nu(^{13}C=O)$, respectively. As expected, the wavenumber of the carbonyl stretching mode is non-sensitive to the different isotopomers of the Se atom.

3.2.1.2. The $\nu_{C=Se}$ region. The $\nu_{C=Se}$ region in the FTIR spectra of OCSe isolated in solid Ar shows a characteristic isotopic pattern depicted in Fig. 4, with absorptions at 648.1 cm^{-1}, 647.0 cm^{-1}, 646.0 cm^{-1}, 643.9 cm^{-1} and 641.8 cm^{-1}, corresponding to ^{76}Se, ^{77}Se, ^{78}Se, ^{80}Se and ^{82}Se, respectively. There are, again, no signs of a matrix effect in this region, in accordance with only one matrix site. In contrast to the carbonylic stretching vibrational mode, which dominates the IR spectrum of carbonyl selenide, the C=Se stretching mode possesses a very low intensity.

3.2.1.3. The $\delta_{O=C=Se}$ region. Two very weak absorptions observed at 466.0 and 464.3 cm^{-1} in the FTIR spectrum of a matrix formed between OCSe and Ar in a proportion of 1:1000 were assigned to the deformation modes of carbonyl selenide. In free OCSe the two deformation modes are degenerated. The presence of two bands, which maintain their relative intensities in all the experimental proportions with the Ar gas used in this study and also after the irradiation of the matrices, is attributed to an asymmetric matrix site, which breaks the degeneracy of the deformation vibrational modes.

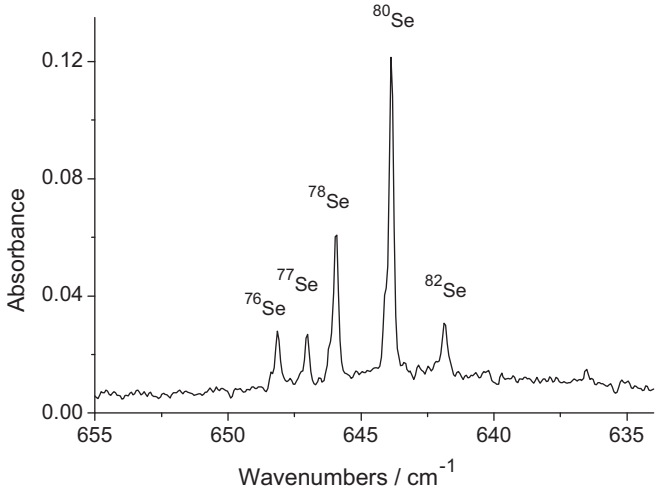

Fig. 4. FTIR spectrum at resolution of 0.125 cm^{-1} in the νC=Se spectral region of OCSe isolated in Ar matrix in an OCSe:Ar 1:1000 proportion.

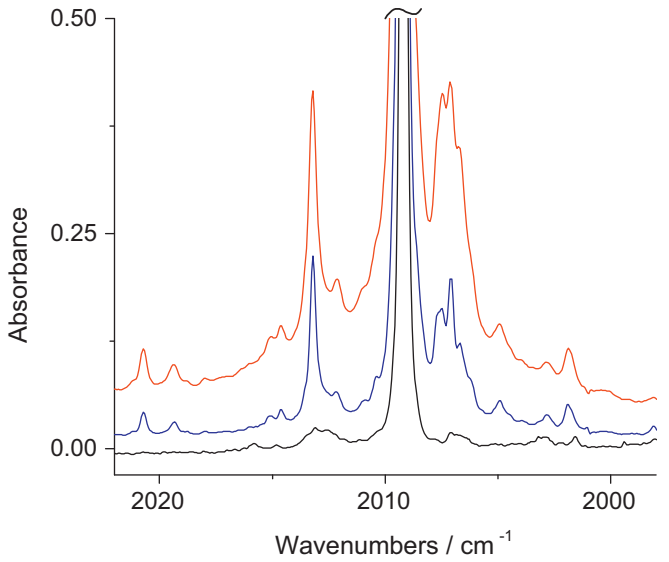

Fig. 5. FTIR spectra in the νC=O spectral region of OCSe isolated in Ar matrix in different OCSe:Ar proportions: from bottom to top 1:1000 (black), 1:500 (blue), and 1:200 (red). (For interpretation of the references to colour in this figure legend, the reader is referred to the web version of the article.)

3.2.1.4. Overtones and combination modes. Table 4 presents a complete list of the overtones and combination bands observable in a matrix of Ar or N_2 containing OCSe. The first overtones of the three vibrational fundamentals, as well as the $\nu_1+\nu_3$ ($\nu_{C=O}+\nu_{C=Se}$) and $\nu_1+2\nu_3$($\nu_{C=O}+2\nu_{C=Se}$) combination modes, are discernible in the Ar matrix spectra.

3.2.2. Dimers of OCSe

As the proportion of OCSe in the mixtures increases, the FTIR spectra change from the simple spectrum of the monomeric OCSe to more complicated spectra which were interpreted in terms of different dimeric structures with the aid of making theoretical predictions. From the theoretical study of the dimeric structures of OCSe presented earlier in this paper, we can conclude that the carbonyl stretching region is by far the most sensitive for the detection of these species.

When the proportion of OCSe in the matrix is increased from 1:1000 to 1:500, several new absorptions appeared in the $\nu_{C=O}$ region of the spectrum, both at higher and lower wavenumbers with respect to the 2009.0 cm^{-1} feature assigned to monomeric OCSe. As can be seen in Fig. 5, the higher the proportion of OCSe in the matrix, the higher the relative intensities of these bands with respect to the $\nu_{C=O}$ of OCSe. The fact that all the absorptions are already present in the 1:500 matrix gives us reason to believe that they arise most plausibly from aggregates of only two molecules. The behaviours of these bands when the matrix is exposed to broadband UV–visible photolysis (see below), together with the results obtained from *ab initio* calculations, give the basis for the tentative assignment of the absorptions to the dimeric structures discussed in Section 3.1.

Table 5
Comparison between the absorptions observed in the IR spectra of OCSe isolated in solid Ar or N_2 in the $\nu_{C=O}$ spectral region and the calculated for monomeric and dimeric species of OCSe using the MP2/aug-cc-pVDZ approximation.

	Ar-matrix		N_2-matrix		MP2/aug-cc-pVDZ	
Species	ν (cm^1)	$\Delta\nu$	ν (cm^1)	$\Delta\nu$	ν (cm^1)	$\Delta\nu$
OCSe	2009.0	–	2015.5	–	2029.6	–
$(OCSe)_2$ I	2020.7	+11.7	2025.4	+9.9	2039.2	+9.6
	2019.4	+10.4				
$(OCSe)_2$ II	2013.3	+4.2	2023.3	+7.8	2035.7	+6.1
	2012.1	+3.1	2020.5	+5.0		
	2002.8	−6.1	2002.1	−13.4	2021.1	−8.5
	2001.9	−7.1				
$(OCSe)_2$ III	2007.5	−1.5	2013.2	−2.3	2027.4	−2.2
$(OCSe)_2$ IV	2010.5	+1.5	2017.8	+2.3	2031.3	+1.7
			2017.5	+2.0		
	2007.1	−1.9	2010.6	−4.9	2026.9	−2.7
	2006.7	−2.3	2009.4	−6.1		
$(OCSe)_2$ V	2004.9	−4.1	2006.9	−8.6	2021.5	−8.1
			2004.9	−10.6		
			2004.4	−11.1		

Table 5 compares the experimental wavenumber shifts observed in the spectra with the calculated for the different dimeric structures using the MP2/aug-cc-pVDZ theoretical approximation. Fig. 6 shows very good agreement between the FTIR spectrum of OCSe isolated in solid Ar in a 1:200 proportion taken with a 0.125 cm^{-1} resolution and the simulated IR spectrum of OCSe in equilibrium with the five dimeric species. For the simulated spectrum, the theoretical expected relative proportion of each of the forms together with the relative absorption coefficients of each of the bands was used.

The C═Se stretching and OCSe deformation vibrational modes of OCSe present very low intensity, making difficult the clear experimental observation of signals attributable to dimeric forms. Anyway, several bands observed as shoulders in the $\nu_{C=Se}$ spectral region and as extremely weak absorptions in the $\delta_{O=C=Se}$ region of the IR spectra of concentrated samples could be tentatively assigned to the different isomers of $(OCSe)_2$. A tentative assignment of the signals observed in the spectra attributable to the dimeric structures is presented in the Supplementary Material in Table S3.

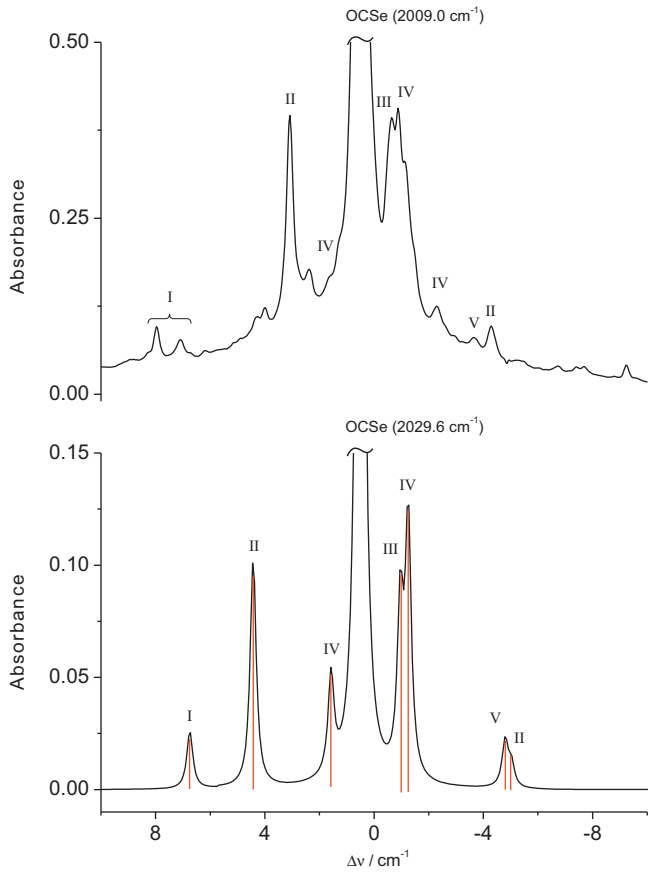

Fig. 6. Comparison between the simulated IR spectrum of a mixtures of monomeric OCSe and the dimeric species $(OCSe)_2$ I–V calculated with the MP2/6-311+G* approximation (bottom) and the FTIR spectra of an Ar matrix of OCSe in a 1:200 proportion at 10 K and 0.125 cm^{-1} resolution (top) in the νC═O spectral region.

3.2.3. Photolysis experiments

OCSe isolated in solid Ar or N_2 matrices was exposed to UV–visible light for different irradiation times. When the 1:1000 OCSe:Ar matrix is irradiated, a new absorption at 2139.7 cm^{-1} is observed to develop in the spectra, as depicted in Fig. 7. The reported value for carbon monoxide isolated in an Ar matrix is 2138.2 cm^{-1} [43,44], and is discernible as a very weak feature in the spectrum of Fig. 7, taken immediately after deposition, due to the thermal decomposition of OCSe before deposition. The

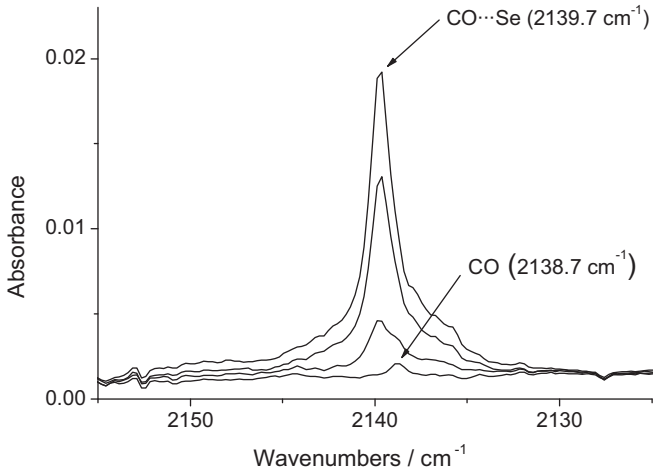

Fig. 7. FTIR spectra of OCSe isolated in solid Ar at 10 K in a 1:1000 proportion in the CO spectral region immediately after deposition and after 10, 30 and 60 s (from bottom to top) of broad-band UV–visible photolysis.

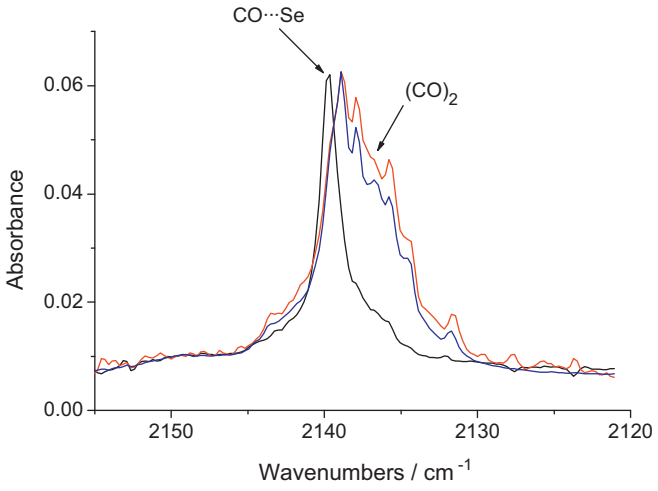

Fig. 8. FTIR spectra of OCSe isolated in solid Ar at 10 K in the CO spectral region in a 1:1000 (black), 1:500 (blue) and 1:200 (red) proportion after 1 min of broad-band UV–visible photolysis. (For interpretation of the references to colour in this figure legend, the reader is referred to the web version of the article.)

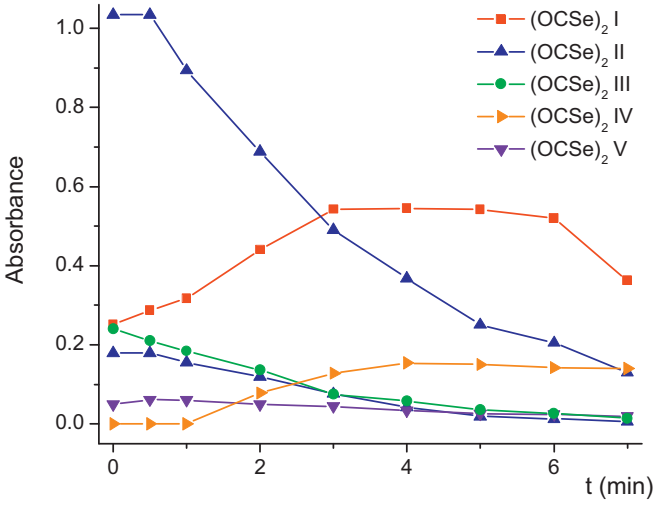

Fig. 9. Plot of the intensities of bands assigned to the dimeric forms of OCSe in the FTIR spectra of an Ar matrix of OCSe in a 1:200 proportion at 10 K *vs* irradiation times (red: 2020.7/2019.4 cm^{-1}; blue: 2013.3/2012.1 and 2002.8/2001.9 cm^{-1}; green: 2007.5 cm^{-1}; orange: 2007.1/2006.7 cm^{-1}; violet: 2004.9 cm^{-1}). (For interpretation of the references to colour in this figure legend, the reader is referred to the web version of the article.)

wavenumber shift observed for the CO absorption when OCSe is irradiated is attributed to a perturbation caused by the Se atom, generated in the same matrix cage (Eq. (1)). This band was already observed during the matrix-isolation reactions between OCSe and F_2 [19], Cl_2 [20] and Br_2 [20].

$$OCSe \xrightarrow[\text{Ar matrix}]{h\nu} CO + Se \quad (1)$$

The IR spectra taken after the photolysis of more concentrated Ar matrices (OCSe:Ar at proportions of 1:500, 1:200 and 1:100) have revealed a more complicated pattern in the region corresponding to the CO molecule, as observed in Fig. 8. The feature formed at 2136.8 cm^{-1} is associated with the CO dimer, $(CO)_2$, by comparison with the reported value isolated in the Ar matrix reported at 2136.7 cm^{-1} [45]. The proposed mechanism for the formation of this species is schematized by Eq. (2)

$$(OCSe)_2 \xrightarrow[\text{Ar matrix}]{h\nu} (CO_2) + 2Se \quad (2)$$

There were no signs in the IR spectra taken after the photolysis of the formation of any other species, including the CO_2 region (~2344 cm^{-1}) [26] and the CSe_2 region (~1300 cm^{-1}) [46]. The distinctive behaviour of the IR bands assigned to monomeric and the different dimeric forms of OCSe against the irradiation times resulted in a very important tool for the correlation of the IR absorption with structures I–V. As shown in Fig. 9, the IR intensities of the features associated with each dimeric form exhibit a different behaviour against the irradiation time. The bands assigned to $(OCSe)_2$ II, which correspond to the most intense dimeric signals in the spectrum taken immediately after deposition, decrease with the irradiation time, while the absorptions attributed to $(OCSe)_2$ I first increase, then remain approximately constant, and in the end begin to decrease. Although the bands assigned to dimers III–V present very low intensities and appear overlapped, which make difficult the measurement of their intensities as the integrated peak areas, the patterns observed in Fig. 9 are clearly different.

The broad-band ($200 \leq \lambda \leq 800$ nm) photolysis of OCSe isolated in an Ar matrix to give CO and Se atoms has proven itself to be a very efficient process. After 2 min photolysis of a matrix containing OCSe:Ar at a proportion of 1:200, approximately 50% of the OCSe is consumed. In similar conditions, the photolysis of matrix-isolated OCS consumes about 25% of the precursor, while matrices containing CO_2 are stable in relation to the irradiation. These behaviours are related with the UV–visible spectra of these molecules in the gas phase, which present absorptions at 250 (OCSe) [9], 224 (OCS) [47] and near to 150 nm (CO_2) [48].

4. Conclusions

The IR spectra of carbonyl selenide isolated in solid Ar or N_2 matrices have revealed the presence of only one matrix site in both solvents. Changes in the spectra with the variation of the OCSe:Ar proportion were tentatively interpreted in terms of different dimeric structures, $(OCSe)_2$. The relative stabilities of these structures and the shifts of the infrared absorptions with respect to monomeric OCSe were reproduced well by quantum chemical calculations. Four of the five proposed structures for $(OCSe)_2$ are in coincidence with reported structures for the $(OCS)_2$ system [29–31]. Additionally, the bonding properties of the molecular complexes were interpreted in terms of the 'donor–acceptor' model. The theoretically most stable form presents a slipped quasi-parallel structure with C_s symmetry, in which the stabilization can be explained through an orbital interaction from a non-bonding orbital of the Se atom of one of the sub-units to a π^*(C=O) orbital of the other sub-unit, and a second contribution from a charge transfer of the π(C=O) bonding orbital of one OCSe molecule to the π^*(C=O) of the other one.

The results of the UV–visible broad-band photolysis of Ar matrices of OCSe reinforce the assignment of the absorptions to the different dimers, as the features corresponding to each structure follow different patterns against in relation to the irradiation time. Mechanisms for the photodecomposition of matrix-isolated OCSe were proposed. Monomeric OCSe decomposes to give CO and Se, as evidenced by the IR absorption of CO perturbed by the presence of a selenium atom in the same matrix cage. Dimeric forms of OCSe originate $(CO)_2$ and Se atoms. The high efficiency observed in the photolysis of OCSe isolated in solid matrices with light of $200 \leq \lambda \leq 800$ nm is in accordance with the high yield of previously studied matrix reactions of halogen molecules with OCSe [19,20].

Acknowledgements

R.M.R. thanks Consejo Nacional de Investigaciones Científicas y Técnicas (CONICET), Facultad de Ciencias Exactas, Universidad Nacional de La Plata, and ANPCyT for financial support. J.A.G.C. acknowledges with thanks a Deutscher Akademischer Austausch Dienst (DAAD) award.

Appendix A. Supplementary data

Supplementary data associated with this article can be found, in the online version, at http://dx.doi.org/10.1016/j.vibspec.2013.10.005.

References

[1] H. Suguro, T. Konno, K. Sueoka, Y. Hamada, H. Uehara, J. Mol. Spectrosc. 124 (1987) 46.
[2] M. Litz, H. Bürger, L.S. Masukidi, A. Fayt, J. Cosléou, P. Dréan, L. Margulés, J. Demaison, J. Mol. Spectrosc. 196 (1999) 155.
[3] K. Sueoka, T. Konno, Y. Hamada, H. Uehara, Chem. Lett. (1986) 1515.
[4] K. Sueoka, Y. Hamada, H. Uehara, J. Mol. Spectrosc. 127 (1988) 370.
[5] H. Bürger, M. Litz, H. Willner, M. LeGuennec, G. Wlodarczak, J. Demaison, J. Mol. Spectrosc. 146 (1991) 220.
[6] Y. Morino, C. Matsumura, Bull. Chem. Soc. Jpn. 40 (1967) 1101.
[7] A.G. Maki, R.L. Sams, R. Pearson, J. Mol. Spectrosc. 64 (1977) 452.
[8] S. Cradock, R.J. Donovan, W. Duncan, H.M. Gillespie, Chem. Phys. Lett. 31 (1975) 344.
[9] M. Bavia, G. Di Lonardo, G. Galloni, A. Trombetti, J. Chem. Soc. Faraday Trans. 68 (1972) 615.
[10] D.C. Frost, S.T. Lee, C.A. McDowell, J. Chem. Phys. 59 (1973) 5484.
[11] S. Cradock, W. Duncan, J. Chem. Soc. Faraday Trans. 71 (1975) 1262.
[12] W.H. Trott, J.R. Woodworth, J.K. Rice, C.K. Miller, J. Appl. Phys. 52 (1981) 5811.
[13] W.K. Bischel, J. Bokor, J. Dallarosa, C.K. Rhodes, J. Chem. Phys. 70 (1979) 5593.
[14] W.K. Bischel, G. Black, R.T. Hawkins, D.J. Kliger, C.K. Rhodes, J. Chem. Phys. 70 (1979) 5589.
[15] G. Black, R.L. Sharpless, T.G. Slanger, J. Chem. Phys. 64 (1976) 3985.
[16] M.J. Shaw, M.C. Gower, S. Rolt, Chem. Phys. Lett. 73 (1980) 478.
[17] M.C. Gower, S. Rolt, C.E. Webb, J. Phys. D: Appl. Phys. 15 (1982) 27.
[18] D.A. Stiles, W.J.R. Tyerman, O.P. Strausz, H.E. Gunning, Can. J. Chem. 44 (1966) 1677.
[19] J.A. Gómez Castaño, A.L. Picone, R.M. Romano, C.O. Della Védova, H. Willner, Chem. Eur. J. 13 (2007) 9355.
[20] J.A. Gómez Castaño, R.M. Romano, H. Willner, C.O. Della Védova, Inorg. Chim. Acta 361 (2008) 540.
[21] J.A. Gómez Castaño, Ph.D. Thesis, University of La Plata, 2009.
[22] S.E. Novick, P.B. Davies, T.R. Dyke, W. Klemperer, J. Am. Chem. Soc. 95 (1973) 8547.
[23] L. Fredin, B. Nelander, G. Ribbegard, J. Mol. Spectrosc. 53 (1974) 410.
[24] K.W. Jucks, Z.S. Huang, R.E. Miller, G.T. Fraser, A.S. Pine, W.J. Lafferty, J. Chem. Phys. 88 (1988) 2185.
[25] K.W. Jucks, Z.S. Huang, D. Dayton, R.E. Miller, W.J. Lafferty, J. Chem. Phys. 86 (1987) 4341.
[26] J.A. Gómez Castaño, A. Fantoni, R.M. Romano, J. Mol. Struct. 881 (2008) 68, and references cited therein.
[27] Y. Ono, E.A. Osuch, C.Y. Ng, J. Chem. Phys. 74 (1981) 1645.
[28] M.A. Hoffbauer, K. Liu, C.F. Giese, W.R. Gentry, J. Phys. Chem. 87 (1983) 2096.
[29] R.W. Randall, J.M. Wilkie, B.J. Howard, J.S. Muenter, Mol. Phys. 69 (1990) 839.
[30] R.G.A. Bone, Chem. Phys. Lett. 206 (1993) 260.
[31] M. Afshari, M. Dehghani, Z. Abusara, N. Moazzen-Ahmadi, A.R.W. McKellar, J. Chem. Phys. 126 (2007) 071102.
[32] A.J. Minei, S.E. Novick, J. Chem. Phys. 126 (2007) 101101.
[33] J. Brown, X.-G. Wang, R. Dawes, T. Carrington, J. Chem. Phys. 136 (2012) 134306.
[34] N. Moazzen-Ahmadi, A.R.W. McKellar, Int. Rev. Phys. Chem. (2013), http://dx.doi.org/10.1080/0144235X.2013.813799.
[35] K. Kondo, S. Yokoyama, N. Miyoshi, S. Murai, N. Sonoda, Angew. Chem. Int. Ed. Engl. 18 (1979) 691.
[36] (a) M.J. Almond, A.J. Downs, Adv. Specrosc. 17 (1989) 1;
(b) I.R. Dunkin, Matrix-Isolation Techniques: A Practical Approach, Oxford University Press, New York, 1998.
[37] R.N. Perutz, J.J. Turner, J. Chem. Soc. Faraday Trans. 69 (1973) 452.
[38] M.J. Frisch, G.W. Trucks, H.B. Schlegel, G.E. Scuseria, M.A. Robb, J.R. Cheeseman, J.A. Montgomery Jr., T. Vreven, K.N. Kudin, J.C. Burant, J.M. Millam, S.S. Iyengar, J. Tomasi, V. Barone, B. Mennucci, M. Cossi, G. Scalmani, N. Rega, G.A. Petersson, H. Nakatsuji, M. Hada, M. Ehara, K. Toyota, R. Fukuda, J. Hasegawa, M. Ishida, T. Nakajima, Y. Honda, O. Kitao, H. Nakai, M. Klene, X. Li, J.E. Knox, H.P. Hratchian, J.B. Cross, V. Bakken, C. Adamo, J. Jaramillo, R. Gomperts, R.E. Stratmann, O. Yazyev, A.J. Austin, R. Cammi, C. Pomelli, J.W. Ochterski, P.Y. Ayala, K. Morokuma, G.A. Voth, P. Salvador, J.J. Dannenberg, V.G. Zakrzewski, S. Dapprich, A.D. Daniels, M.C. Strain, O. Farkas, D.K. Malick, A.D. Rabuck, K. Raghavachari, J.B. Foresman, J.V. Ortiz, Q. Cui, A.G. Baboul, S. Clifford, J. Cioslowski, B.B. Stefanov, G. Liu, A. Liashenko, P. Piskorz, I. Komaromi, R.L. Martin, D.J. Fox, T. Keith, M.A. Al-Laham, C.Y. Peng, A. Nanayakkara, M. Challacombe, P.M.W. Gill, B. Johnson, W. Chen, M.W. Wong, C. Gonzalez, J.A. Pople, Gaussian 03 Revision C.02, Gaussian Inc., Wallingford, CT, 2004.
[39] P.I. Nagy, D.A. Smith, G. Alagona, C. Ghio, J. Phys. Chem. 98 (1994) 486.
[40] S.F. Boys, F. Bernardi, Mol. Phys. 19 (1970) 553.
[41] A. Bondi, J. Phys. Chem. 68 (1964) 441.
[42] A.E. Reed, L.A. Curtiss, F. Weinhold, Chem. Rev. 88 (1988) 899.
[43] H. Dubost, Chem. Phys. 12 (1976) 139.
[44] R.M. Romano, C.O. Della Védova, J. Phys. Chem. A 107 (2003) 5398.
[45] L.M. Nxumalo, E.K. Ngidi, T.A. Ford, J. Mol. Struct. 786 (2006) 168.
[46] S. Li, T.S. Chwee, W.Y. Fan, J. Phys. Chem. A 109 (2005) 11815.
[47] S.P. McGlynn, J.W. Rabalais, J.R. McDonald, V.M. Scherr, Chem. Rev. 71 (1971) 73.
[48] R.J. Jensen, R.D. Guettler, J.L. Lyman, Chem. Phys. Lett. 277 (1997) 356.